Molecular Pharmacology Fast Forward. Published on December 19, 2005 as doi:10.1124/mol.105.018770
This article has not been copyedited and formatted. The final version may differ from this version.

MOL (18770)

Ester Derivatives of Tournefolic Acid B Attenuate N-Methyl-D-Aspartate–Mediated Excitotoxicity in Rat Cortical Neurons

Chuen-Neu Wang, Hsien-Chia Pan, Yun-Lian Lin, Chih-Wen Chi, and Young-Ji Shiao

National Research Institute of Chinese Medicine, Taipei, Taiwan, R.O.C. (C.N.W., Y.L.L., Y.J.S.); Institute of Biopharmaceutical Science (H.C.P., Y.J.S.) and Institute of Pharmacology (C.W.C.), National Yang-Ming University, Taipei, Taiwan, R.O.C.

Molecular Pharmacology Fast Forward. Published on December 19, 2005 as DOI: 10.1124/mol.105.018770
This article has not been copyedited and formatted. The final version may differ from this version.

Running Title: Ester derivatives of tournefolic acid B block NMDA excitotoxicty

Address correspondence to:

Dr. Young-Ji Shiao

National Research Institute of Chinese Medicine

NO. 155-1. Sec. 2, LiNung ST., Peitou, Taipei, Taiwan, R.O.C.

Telephone: (886)-2-2820-1999 ext 4171

Fax: (886)-2-28264266

E-mail: yshiao@nricm.edu.tw

Number of text pages: 34

Number of tables: 0

Number of figures: 11

Number of references: 40

Number of words in the Abstract: 247

Number of words in the Introduction: 585

Number of words in the Discussion: 1112

Abbreviations: AIF, apoptosis-inducing factor; JNK, c-jun N-terminal kinase; MAP2, microtubule-associated protein 2; MTT, 3-[4,5-dimethylthiazol-2-yl]-2,5-diphenyl-tetrazolium bromide; PARP-1, Poly(ADP)-ribose polymerase-1; ROS, reactive oxygen species; TABE, tournefolic acid B ethyl ester; TABM, tournefolic acid B methyl ester; TRAF2, TNF receptor-associated factor 2

Molecular Pharmacology Fast Forward. Published on December 19, 2005 as DOI: 10.1124/mol.105.018770
This article has not been copyedited and formatted. The final version may differ from this version.

ABSTRACT

The effects of tournefolic acid B (TAB) and two ester derivatives, TAB methyl ester (TABM) and TAB ethyl ester (TABE), on N-methyl-D-aspartate (NMDA)-mediated excitotoxicity and the underlying mechanisms were investigated. Treatment with 50 μM NMDA elicited neuronal death by 48.7 ± 5.1% coinciding with the appearance of injured morphology. 50 μM TABM attenuated the NMDA-induced cell death by 60.9 ± 19.7%, and to a lesser extent by TABE. The NMDA-mediated activation of calpain was not affected by TABM and TABE as determined by the cleavage of α-spectrin. NMDA increased the activity of caspase 2, 3, 6, 8, and 9 and reached the maximum after 8 h treatment. TABM and TABE abrogated NMDA-induced activation of caspase 2, 3, 6, and 8 by about 80-90% and 50-60%, respectively, and to a higher extent for caspase 9. TABM and TABE also blocked the NMDA-mediated activation of caspase 12. Furthermore, TABM and TABE eliminated the NMDA-induced accumulation of superoxide anion ($O_2^{\bullet -}$). NMDA evoked significant depolarization of mitochondria, whereas TABM elicited a mild decrease of mitochondrial membrane potential as determined by TMRM. NMDA treatment induced elevation of Ca^{2+} level in cytosol, endoplasmic reticulum (ER), and mitochondria. 50 μM TABM significantly diminished the NMDA-induced elevation of Ca^{2+} level in mitochondria and ER, but not cytosol. Therefore, TABM decreased mitochondrial membrane potential and attenuated the NMDA-mediated Ca^{2+}-loading in ER and mitochondria. These events subsequently

eliminated the accumulation of $O_2^{\bullet -}$ and blocked the activation of caspases cascade, thereby conferring their neuroprotective effects on NMDA-mediated excitotoxicity.

Molecular Pharmacology Fast Forward. Published on December 19, 2005 as DOI: 10.1124/mol.105.018770
This article has not been copyedited and formatted. The final version may differ from this version.

Introduction

Glutamate is an essential mediator of excitotoxicity. The sustained activation of N-methyl-D-aspartate (NMDA) receptor, a subclass of the ionotropic glutamate receptor family, accounts for the majority of glutamate excitotoxicity (Sattler and Tymianski, 2001). Classic morphological studies have documented that necrosis is the predominant lesion of excitotoxicity (Portera-Cailliau et al., 1997). Apoptosis is also involved in excitotoxic neuronal death as an apoptosis-necrosis continuum (Polster and Fiskum, 2004).

Binding of glutamate to NMDA receptors triggers a rapid influx of Ca^{2+} that culminates in neuron death. The extreme overload of Ca^{2+} in neuron and dysfunction of Ca^{2+} extrusion pathway consequently lead to failure of maintaining a low intracellular Ca^{2+} level (Bano et al., 2005). The excessive amount of Ca^{2+} is sequestered by mitochondria and endoplasmic reticulum (ER) (Nicholls and Akerman, 1982). Mitochondria uptake cytoplasmic Ca^{2+} *via* uniporter using proton electrochemical gradient as driving force (Nicholls et al., 2003). The overload of calcium in mitochondria might have detrimental effects due to the enhanced production of reactive oxygen species (ROS), mitochondria depolarization, and bioenergetic failure (Patel et al., 1996; Schinder et al., 1996; White and Reynolds, 1996).

Alteration of Ca^{2+} homeostasis in ER has been reported to render neurons vulnerable to the excitotoxicity (Guo et al., 1999). Sustained elevations of intracellular Ca^{2+} induce apoptosis by activating caspases 12 in a calpain-dependent manner (Nakagawa and Yuan,

2000). Caspase-12 activity is induced by caspase-7 or the Ire1/TNF receptor-associated factor 2 (TRAF2)/c-Jun N-terminal kinase (JNK) complex at the ER membrane. Caspase 12 plays a pivotal role in the progression of ER stress-induced cell death through cleaving procaspase-9 (Nakagawa and Yuan, 2000; Morishima et al., 2002).

Evidence has suggested that one of the most damaging consequences of excessive calcium is the generation of ROS (Coyle and Puttfarcken, 1993). Neurons are especially vulnerable to ROS damage due to their high basal metabolic rate and relatively low levels of antioxidant defense (Halliwell, 1992). Activation of glutamate receptor increases the formation of superoxide anion ($O_2^{\bullet -}$) through a mitochondria-mediated pathway (Patel et al., 1996). Receptor-mediated elevation of Ca^{2+} also promotes the formation of nitric oxide (NO) through neuronal nitric oxide synthase (NOS). Both NO and $O_2^{\bullet -}$ are involved in the neurotoxic process. Furthermore, interaction of $O_2^{\bullet -}$ and NO generates peroxynitrite ion that exhibits a much more damaging effect on neurons. The nuclear translocation of apoptosis-inducing factor (AIF), activation of Poly(ADP)-ribose polymerase-1 (PARP-1) (Yu et al., 2002), and increase in P53 and Bax (Djebaili et al., 2000) are also implicated in the NMDA-induced neuronal apoptosis.

Numerous pieces of evidences have suggested that some antioxidants are capable of inhibiting glutamate-induced neurotoxicity (Lee et al., 2004; Kanada et al., 2005). A variety of polyphenolic compounds have been isolated from *Tournefortia sarmentosa* Lam.

(Boraginaceae) (Chinese name: Teng Zi Dan) widely used in Taiwan as detoxicant and anti-inflammatory agent (Lin et al. 2002). Most of these polyphenolic compounds possess antioxidative activity including tournefolic acid B (TAB), TAB methyl ester (TABM), and TAB ethyl ester (TABE) (Fig. 1). The TAB structure-relative compounds also exhibited neuroprotective potency against glutamate-mediated neurotoxicity (Chi et al., 2005). In the present study, we therefore attempt to investigate the neuroprotective effects of TAB, TABM, and TABE on NMDA-mediated toxicity in primary cultures of rat cortical neurons. The underlying mechanisms following which TAB derivatives confer their effects were also elucidated. The results showed that TABM/TABE decreased mitochondrial membrane potential and attenuated the NMDA-mediated Ca^{2+} stress on ER and mitochondira, subsequently blocked the activation of caspases cascade and eliminated the accumulation of $O_2^{\bullet -}$, thereby conferring their neuroprotective effects on NMDA-mediated neurotoxicity.

Molecular Pharmacology Fast Forward. Published on December 19, 2005 as DOI: 10.1124/mol.105.018770
This article has not been copyedited and formatted. The final version may differ from this version.

Materials and Methods

Materials. All reagents for electrophoresis were purchased from Bio-Rad Laboratories (Hercules, CA, USA). Medium and materials for cell cultures were obtained from Invitrogen (Carlsbad, CA, USA). Enhanced chemiluminescence detection reagents, anti-rabbit IgG antibody conjugated with horseradish peroxidase, and anti-mouse IgG antibody conjugated with horseradish peroxidase were obtained from Amersham Bioscience (Buckinghamshire, UK). NMDA was purchased from Sigma (St. Louis, MO, USA). Fluo-3 AM, rhod-2 AM, mag-fura-2 AM, TMRM, MitoTracker Green FM, ER-tracker Red, and dihydroethidium were purchased from Molecular Probes (Eugene, OR, USA). Monoclonal anti-microtubule-associated protein 2 (MAP2) and anti-α-spectrin antibodies were obtained from Upstate (Charlottesville, VA, USA) and Chemicon (Temecula, CA, USA), respectively. Polyclonal anti-caspase 12 antibody was purchased from BioVision (Mountain View, CA, USA). Colorimetric substrates for caspases were obtained from BioSourse (Nivelles, Belgium). All other reagents were purchased from Sigma (St. Louis, MO, USA) or Merck (Darmstadt, Germany).

Extraction and isolation. Stems of *T. samentosa* Lam. were collected from Nei-Men, Kaohsiung County, Taiwan, in August 1998. The plant was identified by comparison with voucher specimens deposited earlier at the Herbarium of Department of Botany, National Taiwan University, Taipei, Taiwan (no. TAI175693, collected April 1, 1979). The extraction

of *T. samentosa* and the isolation and purification of bioactive polyphenolic compounds were described previously (Lin et al., 2002). TABM was the derivative of TAB during the hot-methanol extraction. The purity of all compounds was greater than 95% using HPLC analysis.

Cell culture. Primary cultures of neonatal cortical neurons were prepared as described previously (Wang et al., 2001). The Institutional Animal Care and Use Committee at the National Research Institute of Chinese Medicine had approved the animal protocol. Briefly, the cortex isolated from Sprague-Dawley rat pup by decapitation was digested in 0.5 mg/ml papain at 37°C for 15 min. The tissue was dissociated in Hibernate A medium (containing B27 supplement) by aspirating trituration. Cells were plated and maintained in Neurobasal medium containing B27 supplement, 10 units/ml penicillin, 10 μg/ml streptomycin, and 0.5 μg/ml glutamine for 3 days. Cells were then exposed to cytosine-β-D-arabinofuranoside (5 μM) for 1 day to eliminate proliferation of non-neuronal cells. The cells were used for experiments on the tenth day.

Treatment of NMDA and ester derivatives of TAB. Cortical neurons were pretreated with vehicle (0.1% dimethyl sulfoxide, DMSO), TABM, TABE, or TAB for 30 min. After then, NMDA was added directly into medium (containing vehicle, TAB, or the ester derivatives of TAB) to a final concentration of 50 μM and incubated for certain period.

Measurement of cell viability. The reduction of 3-[4,5-dimethylthiazol-2-yl]-2,5-diphenyl-tetrazolium bromide (MTT) and release of lactate dehydrogenase (LDH) were

Molecular Pharmacology Fast Forward. Published on December 19, 2005 as DOI: 10.1124/mol.105.018770
This article has not been copyedited and formatted. The final version may differ from this version.

employed to evaluate the cell viability. Cells were incubated with 0.5 mg/ml MTT for 1 h. The formazan particle was dissolved with DMSO. $O.D._{600\ nm}$ was measured by using ELISA reader. The activity of LDH was determined by the method described previously (Roth et al., 1999).

Immunocytochemistry. Treated cells were fixed with 4% paraformaldehyde at room temperature for 15 min and permeabilized with 0.5% Triton X-100 for 10 min. Cells were blocked with 10 % control donkey serum at room temperature for 2 h. Thereafter, cells were exposed to anti-MAP2 monoclonal antibody (1:100 dilution) at 4°C overnight. After wash, donkey anti-mouse IgG antibody conjugated with fluorescein (20 μg/ml) was applied to cells and incubated at 37°C for 1 h. Coverslips were mounted onto glass slides and detected by Leica CS SP confocal fluorescence microscope (Wetzlar, Germany).

Measurement of superoxide anion ($O_2^{\bullet-}$). Intracellular level of $O_2^{\bullet-}$ was measured by dihydroethidium assay (Zhang et al., 2003). Treated cells were loaded with 3.2 μM dihydroethidium at 37°C for 30 min then observed by Leica DMIRB fluorescence microscope. The intensity of fluorescence in nuclear position was measured by using MetaMorph software (Universal Imaging Co., West Chester, PA, USA).

Measurement of cellular activity of caspases. Treated cells were harvested in cell lysis buffer (50 mM Hepes pH 7.4, 1 mM dithiothreitol, 0.1 mM EDTA, 0.1% Chaps, and 0.1% Triton X-100). The cellular lysates were prepared and subjected to assay of caspases activity.

Molecular Pharmacology Fast Forward. Published on December 19, 2005 as DOI: 10.1124/mol.105.018770
This article has not been copyedited and formatted. The final version may differ from this version.

Intracellular activity of caspase 2, 3, 6, 8, and 9 was determined by the ability to cleavage Ac-VDVAD-pNA, Ac-DEVD-pNA, Ac-VEID-pNA, Ac-IETD-pNA, and Ac-LEHD-pNA, respectively. The detailed experiments were performed according to the manufacture's protocol. Immunobloting was performed to verify the activation of caspase 12 by the disappearance of procaspase 12 (40 KDa).

Immunobloting. Treated cells were washed twice with ice-cold PBS and collected in harvest buffer (50 mM Hepes pH 7.5, 2.5 mM EDTA, 1 μM PMSF, 10 μg/ml aprotinin, and 10 μg/ml leupeptin). The cellular lysates were prepared and subjected to SDS-polyacrylamide gel electrophoresis (SDS-PAGE) and immunobloting. Rabbit anti-caspase 12 antibody (1:3000 dilution) and mouse anti-α-spectrin antibodies (1:3000 dilution) were used to detect the intracellular level of procaspase 12 and α-spectrin, respectively. Fujifilm LAS-3000 (Tokyo, Japan) was used to detect and quantify the immunoreactive protein.

Determination of mitochondrial membrane potential. Cells were loaded with 100 nM TMRM at 37°C for 20 min. After wash with Hanks' balanced salt solution (HBSS) (137 mM NaCl, 5.4 mM KCl, 0.4 mM KH_2PO_4, 4.2 mM $NaHCO_3$, 0.5 mM $MgCl_2$, 0.6 mM $MgSO_4$, and 5.6 mM D-glucose, pH7.4), cells were incubated in HBSS containing 2 mM $CaCl_2$ and transferred to a microscope-equipped humidity chamber in a condition of 37°C and 5% CO_2. 50μM NMDA or 50μM TABM were added into cell culture at 3 min time-point and incubated for 27 min. The fluorescence of TMRM was detected by Leica DMIRB

Molecular Pharmacology Fast Forward. Published on December 19, 2005 as DOI: 10.1124/mol.105.018770
This article has not been copyedited and formatted. The final version may differ from this version.

fluorescence microscope with excitation wavelength 555 nm. The time-lapse images during 30 min were captured every 15 sec using MetaFluor software (Universal Imaging Co., West Chester, PA, USA).

Measurement of intracellular, mitochondria, and ER calcium. Intracellular free Ca^{2+} ($[Ca^{2+}]_i$) was measured using fluo-3 AM. Cells were loaded with 1 μM fluo-3 AM at 37°C for 15 min. Cells were washed with HBSS and incubated in HBSS containing 2 mM $CaCl_2$. Cells were treated with vehicle or 50 μM TABM at 37°C for 30 min then transferred to a microscope-equipped humidity chamber in a condition of 37°C and 5% CO_2. Cells were exposed to 50 μM NMDA and detected by Leica DMIRB fluorescence microscope with excitation wavelength 484 nm. Free Ca^{2+} in mitochondria ($[Ca^{2+}]_{mit}$) was quantified using rhod-2 AM. The cells were loaded with 1 μM rhod-2 AM at 37°C for 15 min. Cells were treated with vehicle or TABM as described above. Cells were transferred to humidity chamber then exposed to NMDA and detected by fluorescence microscope with excitation wavelength 555 nm. Free Ca^{2+} in ER ($[Ca^{2+}]_{er}$) was determined by mag-fura-2 AM. Cells were loaded with 5 μM mag-fura-2 AM at 37°C for 60 min. Cells were incubated in Mg^{2+}-free HBSS containing 2 mM $CaCl_2$ and treated with vehicle or TABM as described above. Cells were transferred to humidity chamber then exposed to NMDA and detected by fluorescence microscope with dual excitation wavelength 340 and 380 nm. The time-lapse images during 60 min were captured every 15 sec using MetaFluor software. The validity of

Molecular Pharmacology Fast Forward. Published on December 19, 2005 as DOI: 10.1124/mol.105.018770
This article has not been copyedited and formatted. The final version may differ from this version.

using mag-fura-2 and rhod-2 to measure $[Ca^{2+}]_{er}$ and $[Ca^{2+}]_{mit}$ was confirmed by the co-localization with ER and mitochondria tracker, respectively.

Statistic analysis. Results are expressed as mean ± S.D. and were analyzed by ANOVA with post hoc multiple comparisons with a Bonferroni test

Molecular Pharmacology Fast Forward. Published on December 19, 2005 as DOI: 10.1124/mol.105.018770
This article has not been copyedited and formatted. The final version may differ from this version.

Results

TABM and TABE differentially blocked the NMDA-mediated excitotoxicity. 50 μM NMDA elicited cell death by 48.7 ± 5.1% as measured by MTT reduction (Figs. 2A-C). NMDA also elevated the LDH release to 35.6 ± 2.2% of total LDH in control cells (Fig. 2D). NMDA provoked cell death coincided with the appearance of discontinuous neurites and MAP-2 collapse (Fig. 2E) (Faddis et al., 1997). The effects of TAB and its ester derivatives, TABM and TABE, on NMDA-induced neurotoxicity were investigated. Results showed that TAB, TABM, and TABE did not alter the MTT reduction (data not shown), LDH release, and MAP-2 staining of cortical neurons. TAB failed to ameliorate the detrimental effect of NMDA on either MTT reduction or LDH release (Figs. 2A, 2D). However, TABM significantly attenuated the NMDA-mediated neurotoxicity in a concentration-dependent manner. TABE also exhibited similar neuroprotective effect on the NMDA-induced neurotoxicity (Figs. 2B, 2C). TABM at 20, 50, and 100 μM abrogated the cell death by 18.0 ± 11.7, 60.9 ± 19.7 and 97.5 ± 21.6%, respectively as measured by MTT reduction. The equivalent values for TABE were 33.3 ± 13.2, 58.9 ± 14.5, and 74.1 ± 3.3%. 50 μM TABM and TABE decreased the LDH release by 50.8 ± 14.4 and 36.2 ± 7.0%, respectively (Fig. 2D). The NMDA-induced neurites breakage and MAP-2 collapse were also abolished by TABM and TABE (Fig. 2E).

Molecular Pharmacology Fast Forward. Published on December 19, 2005 as DOI: 10.1124/mol.105.018770
This article has not been copyedited and formatted. The final version may differ from this version.

TABM and TABE abrogated the NMDA-induced activation of caspases. Treatment with NMDA induced the activation of calpain and caspase 3 as determined by the degradation of α-spectrin (Fig. 3) (Pang et al., 2003). The activation of calpain produced 145 and 150 KDa fragments of α-spectrin, whereas activation of caspase 3 generated 120 and 150 KDa fragments of α-spectrin. Both 150 KDa and 145 KDa protein fragments appeared at 30-60 min after exposure to 50 μM NMDA (Figs. 3C, 3D). The 120 KDa degraded fragment only significantly generated after 4-30 h (Fig. 3E). The generation of degraded α-spectrin fragments was in parallel to the disappearance of 250 KDa α-spectrin in a time-dependent manner (Fig. 3B). TABM and TABE did not show any effects on the activation of calpain (Figs. 4C, 4D). 50 μM TABM reduced the NMDA-mediated production of 120 KDa by 37.6 ± 7.1 and 25.3 ± 1.6% at 8 and 24 h, respectively (Fig. 4E). TABM attenuated the production of 120 KDa coincided with the accumulation of 250 KDa at 8 and 24 h (Fig. 4B). 50 μM TABM and TABE diminished the degradation of α-spectrin by 63.2 ± 12.6 and 35.8 ± 0.7% at 24 h, respectively.

The *in vitro* assay was further conducted to evaluate the effects of TABM and TABE on the activity of caspases. NMDA treatment increased the caspase activity in a time-dependent manner and reached the maximum at 8 h (Fig. 5A). Treatment with 50 μM NMDA for 8 h increased the activity of caspase 2, 3, 6, and 8 to 9.7 ± 2.1, 7.2 ± 0.4, 7.3 ± 2.8, and 3.0 ± 0.7-fold of control, respectively. The activity of caspase 9 was barely detected in control cells.

Molecular Pharmacology Fast Forward. Published on December 19, 2005 as DOI: 10.1124/mol.105.018770
This article has not been copyedited and formatted. The final version may differ from this version.

NMDA treatment elevated the activity of caspase 9 to a maximum at 8 h. 50 μM TABM attenuated the NMDA-mediated activity of caspase 2, 3, 6, 8, and 9 by 87.6 ± 13.5, 78.3 ± 10.6, 76.5 ± 14.1, 89.1 ± 18.8, and 101.8 ± 3.7% at 8 h, respectively (Fig. 5B). The equivalent values for TABE were 50.4 ± 14.5, 48.9 ± 9.9, 49.2 ± 10.1, 59.6 ± 13.6, and 78.3 ± 12.7%.

The activity of caspase 12 was also verified by the cleavage of procaspase 12 (Fig. 6). The results showed that NMDA induced the cleavage of 40 KDa procaspase 12 but not the 55 KDa procaspase 12 in a time-dependent manner (Fig. 6A). Treatment with 50 μM TABM and TABE for 8 h decreased the NMDA-induced cleavage of 40 KDa procaspase 12 by 46.3 ± 10.3 and 39.3 ± 7.5%, respectively (Fig. 6B).

TABM and TABE blocked the NMDA-induced accumulation of $O_2^{\bullet-}$. Dihydroethidium was used to measure the intracellular level of $O_2^{\bullet-}$. Treatment with NMDA significantly provoked $O_2^{\bullet-}$ accumulation from 10 to 30 min (Fig. 7A). Treatment with 50 μM NMDA for 10, 20, and 30 min elevated the level of $O_2^{\bullet-}$ to 209.7 ± 35.1, 466.8 ± 45.5, and 217.8 ± 58.8% of control, respectively. 50 μM TABM and TABE diminished the NMDA-induced $O_2^{\bullet-}$ accumulation by 86.6 ± 11.0 and 68.2 ± 26.5% at 20 min, respectively (Fig 7B).

TABM decreased the mitochondrial membrane potential. TMRM was used to verify whether TABM directly modulated the mitochondrial membrane potential. The change profile of fluorescence after exposure to NMDA or TABM was similar during cell population

Molecular Pharmacology Fast Forward. Published on December 19, 2005 as DOI: 10.1124/mol.105.018770
This article has not been copyedited and formatted. The final version may differ from this version.

in spite of the heterogeneous fluorescence intensity of each individual cell (Fig. 8). 50 μM NMDA induced a slight decline of TMRM fluorescence at 0.5 min. A marked mitochondria depolarization occurred after 1 min and reached the plateau at about 10 min. In contrast to NMDA, TABM elicited significant mitochondria depolarization immediately. Treatment with 50 μM TABM for 0.5 min reduced the fluorescence intensity by 22.3 ± 4.6 %. However, TABM-induced mitochondria depolarization was much slower than NMDA after 1 min. Treatment with NMDA and TABM for 7 min decreased the fluorescence intensity by 63.3 ± 4.2 and 41.8 ± 5.3%, respectively. Nevertheless, there was no significant difference in fluorescence intensity between cells treated with NMDA and TABM after 20 min.

TABM attenuated the NMDA-induced increase of Ca^{2+} level in ER and mitochondria. Fluo-3, mag-fura-2, and rhod-2 were employed to determine the level of free Ca^{2+} in cytosol, ER, and mitochondria, respectively. 50 μM NMDA immediately elevated the fluorescence intensity of fluo-3 to 1.53 ± 0.32-fold of initial at 5 min, and the fluorescence intensity was maintained to 30 min following by a slight decline (Fig. 9). TABM slightly decreased the initial rate of NMDA-induced elevation of fluo-3 fluorescence. However, TABM elevated the fluorescence intensity to 1.93 ± 0.29 and 1.87 ± 0.11-fold of initial at 30 and 60 min, respectively.

NMDA treatment rapidly increased the level of $[Ca^{2+}]_{er}$. The ratiometric value of mag-fura-2 was increased from 0.19 ± 0.05 to 0.47 ± 0.07 and 0.69 ± 0.04 for 5 and 30 min,

Molecular Pharmacology Fast Forward. Published on December 19, 2005 as DOI: 10.1124/mol.105.018770
This article has not been copyedited and formatted. The final version may differ from this version.

respectively (Fig. 10). Treatment with 50 μM TABM significantly attenuated the NMDA-mediated elevation of ratiometric value to 0.28 ± 0.14 and 0.39 ± 0.06 for 5 and 30 min, respectively. Nevertheless, there was no significant difference in ratiometric value between control and TABM-treated cells at 60 min.

The fluorescence of rhod-2 was elevated by NMDA to 2.17 ± 0.15, 3.02 ± 0.19, and 2.98 ± 0.09-fold of initial fluorescence intensity for 5, 30, and 60 min, respectively (Fig. 11). Treatment with 50 μM TABM diminished the basal fluorescence intensity by about 50%. TABM caused a delayed increase of rhod-2 fluorescence and reached the maximum at 30 min. The NMDA-mediated elevation of fluorescence intensity was also abrogated by TABM.

Molecular Pharmacology Fast Forward. Published on December 19, 2005 as DOI: 10.1124/mol.105.018770
This article has not been copyedited and formatted. The final version may differ from this version.

Discussion

In the present study, we demonstrated that TABM and TABE, but not TAB, abrogated NMDA-mediated excitotoxicity as determined by MTT reduction, LDH release and morphological observation. TABM decreased mitochondrial membrane potential in parallel to attenuating the NMDA-mediated Ca^{2+}-loading in ER and mitochondria. TABM and TABE diminished the accumulation of $O_2^{\bullet -}$, blocked activation of the caspase cascade, and thereby protected neuron against NMDA-mediated neurotoxicity.

Both necrosis and apoptosis are implicated in excitotoxicity (Portera-Cailliau et al., 1997; Polster and Fiskum, 2004). Necrosis is characterized by the irreversible swelling of cytoplasm and its organelles. Loss of membrane integrity results in cell lysis and the release of noxious cellular constituents. Recent study has suggested that calpain is involved in the necrotic and apoptotic processes during excitotoxicity (Wang, 2000; Pang et al., 2003). There are two isoforms of calpain named μ-calpain and m-calpain. μ-calpain and m-calpain requires micromolar or milimolar of Ca^{2+} level for the activation, respectively. Our results showed that NMDA triggered the leakiness of LDH, indicating that a necrotic event is involved in NMDA-mediated excitotoxicity. TABM and TABE significantly abrogated NMDA-mediated neuron necrosis as measured by LDH release. However, neither TABM nor TABE affected the NMDA-mediated activation of calpain. These results suggest that TABM and TABE might modulate other mechanisms to confer their anti-necrotic effects. The study

Molecular Pharmacology Fast Forward. Published on December 19, 2005 as DOI: 10.1124/mol.105.018770
This article has not been copyedited and formatted. The final version may differ from this version.

of Adamec et al. also showed that calpain I activation in rat hippocampal neurons is NMDA receptor selective but not essential for excitotoxic cell death (Adamec et al., 1998).

Apoptosis-mediated cell death in excitotoxicity has become the focus of intense interest. However, the underlying mechanisms remain unclear. Studies have shown that glutamate activates caspase 3 in cultured cortical neurons, striatal neurons, and mesencephalic neurons (Liu and Zhu, 1999; Madhavan et al., 2003). Our previous study also demonstrates that glutamate ubiquitously elicits the activation of caspase 2, 3, 6, 8, and 9 (Chi et al., 2005). The present study further provided evidence that NMDA extensively activated the initiative caspases (i.e. caspase 2, 8, 9, and 12) and the executive caspases (i.e. caspase 3 and 6). The attenuation of NMDA-induced activation of caspase activity may, at least in part, account for the neuroprotective effect of TABM and TABE.

Glutamate triggers a massive influx of Ca^{2+} *via* ionotropic receptor into the intracellular compartment. ER and mitochondria function as the intracellular stores to sequester the excessive amount of cytosolic Ca^{2+}. It is well established that the disturbance of Ca^{2+} homeostasis in mitochondria ultimately causes the deregulation of ROS production and bioenergetic metabolism. Mitochondrion is the main target compartment for multiple anti-apoptotic and pro-apoptotic molecules such as Bcl2, Bax, Bad, Bid, etc. Furthermore, mitochondrion is involved in the activation of caspase 9 mediating by cytochrome c release. Therefore, mitochondrion is a pivotal organelle implicating in apoptosis (Polster and Fiskum,

Molecular Pharmacology Fast Forward. Published on December 19, 2005 as DOI: 10.1124/mol.105.018770
This article has not been copyedited and formatted. The final version may differ from this version.

2004). Recently, ER has attracted attention as an intracellular compartment in which disturbance of calcium homeostasis may contribute to pathological processes culminating in neuronal injury (Mattson et al., 2000; Paschen, 2001; Scorrano et al., 2003). Calcium levels in ER are several orders of magnitude higher than that in cytoplasm. ER calcium homeostasis is controlled by the ryanodine receptor (RyaR) and IP3 receptor (IP3R), which release calcium ions from ER stores upon activation, and the calcium pump (SERCA) which pumps back calcium ions against a steep concentration gradient.

Treatment with glutamate or NMDA evokes a rapid rise in $[Ca^{2+}]_i$ which then shows a second phase of Ca^{2+} elevation (Duchen, 2000; Pivovarova et al., 2004; Bano et al., 2005). Glutamate-induced initial calcium spike is mainly due to the calcium influx through NMDA receptor-gated channel. The influx of calcium through voltage-gated calcium channels and calcium intake due to the reverse mode of the Na^+/Ca^{2+} exchanger may also partly contribute to the initial calcium increase (Thmianski et al., 1993). Our unpublished data showed that change of $[Ca^{2+}]_i$ was barely detected when the experiment was conducted using calcium-free buffer. Therefore, the release of calcium from intracellular stores may be not involved in the initial increase of $[Ca^{2+}]_{i.}$ induced by NMDA. The delayed increase of $[Ca^{2+}]_i$ is proposed to be the consequence of influx of Ca^{2+}, outflow of Ca^{2+} from mitochondria, and calpain-dependent cleavage of Na^+/Ca^{2+} exchanger (Randall and Thayer, 1992; Duchen, 2000; Bano et al., 2005). The present study showed that the profile of $[Ca^{2+}]_i$ displayed a mixed pattern

Molecular Pharmacology Fast Forward. Published on December 19, 2005 as DOI: 10.1124/mol.105.018770
This article has not been copyedited and formatted. The final version may differ from this version.

rather than a typical two phase elevation of Ca^{2+}. It is conceivable that the outflow of $[Ca^{2+}]_i$ from mitochondria may be faster in our system. This speculation is supported by the result of mitochondrial membrane potential. NMDA elicited rapid depolarization of mitochondria subsequently leading to the release of $[Ca^{2+}]_i$ from mitochondria. Treatment with TABM caused a higher level of $[Ca^{2+}]_i$ after 15 min comparing to the control cells. The result suggests that TABM might retard the entrance of Ca^{2+} into mitochondria or ER. This assumption is further confirmed by the results of $[Ca^{2+}]_{er}$ and $[Ca^{2+}]_{mito}$. NMDA elicited significant elevation of $[Ca^{2+}]_{er}$ and $[Ca^{2+}]_{mit}$. Cell treated with TABM exhibited a delayed increase of $[Ca^{2+}]_{er}$. Individual TABM-treated cell exerted heterogeneous time-course of delayed increase of $[Ca^{2+}]_{er}$. For $[Ca^{2+}]_{mit}$, TABM delayed the time-course of increase of $[Ca^{2+}]_{mit}$ and decreased the extent of maximum value. Therefore, the increased level of $[Ca^{2+}]_i$ in TABM-treated cells may reflect the impairment of Ca^{2+} sequestrating by ER and mitochondria. Furthermore, the relevance of delayed increase of $[Ca^{2+}]_{er}$ and attenuate elevation of $[Ca^{2+}]_{mit}$ on the neuroprotection is supported by the subsequent anti-apoptotic events. These events include the diminishment of ER-related activation of caspase 12, abolishment of mitochontria-mediated accumulation of $O_2^{\bullet-}$, and blockade of mitochondria-involved activation of caspase 9 and caspase 3.

The Ca^{2+} homeostasis of ER is maintained by the balance between RyaR/IP3R-mediated release of Ca^{2+} and SERCA-related pump in of Ca^{2+}. The TABM-mediated

Molecular Pharmacology Fast Forward. Published on December 19, 2005 as DOI: 10.1124/mol.105.018770
This article has not been copyedited and formatted. The final version may differ from this version.

depolarization of mitochondria may be concomitant with the depletion of ATP (Starkov et al, 2004), thereby impairing ATP dependent processes of ER Ca^{2+} accumulation (via SERCA). This may provide an explanation for the modulation of Ca^{2+} homeostasis in ER by TABM. Several studies have provided evidences that mild decrease in mitochondrial membrane potential impairs the uptake of Ca^{2+}, in turn protects neuron from cell death (Stout et al., 1998; Mattiasson et al., 2003; Pivovarova et al., 2004; Marks et al., 2005). Our results also demonstrated that TABM decreased mitochondrial membrane potential. The depolarization of mitochondria is associated with decreasing ROS production and blocking mitochondrial Ca^{2+} uptake (Starkov et al, 2004). This explains the result that the basal level of $[Ca^{2+}]_{mit}$ was prominently reduced by TABM. These results clearly demonstrated that TABM/TABE decreased mitochondrial membrane potential and attenuated the Ca^{2+}-overload in both mitochondria and ER, consequently impaired NMDA-induced activation of caspases cascade and eliminated the accumulation of $O_2^{\bullet -}$, thereby conferring their neuroprotective effects on NMDA-mediated neurotoxicity.

References

Adamec E, Beermann ML and Nixon RA (1998) Calpain I activation in rat hippocampal neurons in culture is NMDA receptor selective and not Essential for Excitotoxic Cell Death. *Brain Res Mol Brain Res* 54:35-48.

Bano D, Young KW, Guerin CJ, Lefeuvre R, Rothwell NJ, Naldini L, Rizzuto R, Carafoli E and Nicotera P (2005) Cleavage of the plasma membrane Na+/Ca2+ exchanger in excitotoxicity. *Cell* 120:275-285.

Chi CW, Wang CN, Lin YL, Chen CF and Shiao YJ (2005) Tournefolic acid B methyl ester attenuates glutamate-induced toxicity by blockade of ROS accumulation and abrogating the activation of caspases and JNK in rat cortical neurons. *J Neurochem* 92:692-700.

Coyle JT and Puttfarcken P (1993) Oxidative stress, glutamate, and neurodegenerative disorders. *Science* 262:689-695.

Djebaili M, Rondouin G, Baille V and Bockaert J (2000) P53 and Bax implication in NMDA induced-apoptosis in mouse hippocampus. *Neuroreport* 11:2973-2976.

Duchen MR (2000) Mitochondria and calcium: from cell signalling to cell death. *J Physiol* 529.1:57-68 57.

Faddis BT, Hasbani MJ and Goldberg MP (1997) Calpain activation contributes to dendritic remodeling after brief excitotoxic injury in vitro. *J Neurosci* 17:951-959.

Guo Q, Fu W, Sopher BL, Miller MW, Ware CB, Martin GM and Mattson MP (1999) Increased vulnerability of hippocampal neurons to excitotoxic necrosis in presenilin-1 mutant knock-in mice. *Nat Med* 5:101-106.

Halliwell B (1992) Reactive oxygen species and the central nervous system. *J Neurochem* 59:1609-1623.

Kanada A, Nishimura Y, Yamaguchi JY, Kobayashi M, Mishima K, Horimoto K, Kanemaru K and Oyama Y (2005) Extract of Ginkgo biloba leaves attenuates kainate-induced increase in intracellular Ca2+ concentration of rat cerebellar granule neurons. *Biol Pharm Bull* 28:934-936.

Lee H, Bae J H and Lee S R (2004) Protective effect of green tea polyphenol EGCG against neuronal damage and brain edema after unilateral cerebral ischemia in gerbils. *J Neurosci Res* 77:892-900.

Tymianski M, Charlton MP, Carlen PL and Tator CH (1993) Source specificity of early calcium neurotoxicity in cultured embryonic spinal neurons. *J Neurosci* 13:2085-2104.

Lin YL, Chang YY, Kuo YH and Shiao MS (2002) Anti-lipid-peroxidative principles from *Tournefortia Sarmentosa*. *J Nat Prod* 65:745-747.

Liu X and Zhu XZ (1999) Roles of p53, c-Myc, Bcl-2, Bax and caspases in glutamate-induced neuronal apoptosis and the possible neuroprotective mechanism of basic fibroblast growth factor. *Brain Res Mol Brain Res* 71:210-216.

Madhavan L, Freed WJ, Anantharam V and Kanthasamy AG (2003) 5-Hydroxytryptamine 1A receptor activation protects against N-methyl-D-aspartate-induced apoptotic cell death in striatal and mesencephalic cultures. *J Pharmacol Exp Ther* 304:913-923.

Marks JD, Boriboun C and Wang J (2005) Mitochondrial nitric oxide mediates decreased vulnerability of hippocampal neurons from immature animals to NMDA. *J Neurosci* 25:6561-6575.

Mattiasson G, Shamloo M, Gido G, Mathi K, Tomasevic G, Yi S, Warden CH, Castilho RF, Melcher T, Gonzalez-Zulueta M, Nikolich K and Wieloch T (2003) Uncoupling protein-2 prevents neuronal death and diminishes brain dysfunction after stroke and brain trauma. *Nat Med* 9:1062-1068.

Mattson MP, LaFerla FM, Chan SL, Leissring MA, Shepel PN and Geiger JD (2000) Calcium signaling in the ER: its role in neuronal plasticity and neurodegenerative disorders. *Trends Neurosci* 23:222-229.

Morishima N, Nakanishi K, Takenouchi H, Shibata T and Yasuhiko Y (2002) An endoplasmic reticulum stress-specific caspase cascade in apoptosis. Cytochrome c-independent activation of caspase-9 by caspase-12. *J Biol Chem* 277:34287-34294.

Nakagawa T and Yuan J (2000) Cross-talk between two cysteine protease families. activation of caspase-12 by calpain in apoptosis. *J Cell Biol* 150:887-894.

Nicholls D and Akerman K (1982) Mitochondrial calcium transport. *Biochim Biophys Acta* 683:57-88.

Nicholls DG, Vesce S, Kirk L and Chalmers S (2003) Interactions between mitochondrial bioenergetics and cytoplasmic calcium in cultured cerebellar granule cells. *Cell Calcium* 34:407-424.

Pang Z, Bondada V, Sengoku T, Siman R and Geddes JW (2003) Calpain facilitates the neuron death induced by 3-nitropropionic acid and contributes to the necrotic morphology. *J Neuropathol Exp Neurol* 62:633-643.

Paschen W (2001) Dependence of vital cell function on endoplasmic reticulum calcium levels: implications for the mechanisms underlying neuronal cell injury in different pathological states. *Cell Calcium* 29:1-11.

Patel M, Day BJ, Crapo JD, Fridovich I and McNamara JO (1996) Requirement for superoxide in excitotoxic cell death. *Neuron* 16:345-355.

Pivovarova NB, Nguyen HV, Winters CA, Brantner CA, Smith CL and Andrews SB (2004) Excitotoxic calcium overload in a subpopulation of mitochondria triggers selayed seath in hippocampal neurons. *J Neurosci* 24:5611-5622.

Polster BM and Fiskum G (2004) Mitochondrial mechanisms of neural cell apoptosis. *J Neurochem* 90:1281-1289.

Portera-Cailliau C, Price DL and Martin LJ (1997) Excitotoxic neuronal death in the immature brain is an apoptosis-necrosis morphological continuum. *J Comp Neurol* 378:70-87.

Randall RD and Thayer SA (1992) Glutamate-induced calcium transient triggers delayed calcium overload and neurotoxicity in rat hippocampal neurons. *J Neurosci* 2:1882-l 895.

Roth A, Schaffner W and Hertel C (1999) Phytoestrogen kaempferol (3,4',5,7-tetrahydroxyflavone) protects PC12 and T47D cells from beta-amyloid-induced toxicity. *J Neurosci Res* 57:399-404.

Sattler R and Tymianski M (2001) Molecular mechanisms of glutamate receptor-mediated excitotoxic neuronal cell death. *Mol Neurobiol* 24:107-29.

Schinder AF, Olson EC, Spitzer NC and Montal M (1996) Mitochondrial dysfunction is a primary event in glutamate neurotoxicity. *J Neurosci* 16:6125-6133.

Scorrano L, Oakes SA, Opferman JT, Cheng EH, Sorcinelli MD, Pozzan T and Korsmeyer SJ (2003) BAX and BAK regulation of endoplasmic reticulum Ca2+: a control point for apoptosis. *Science* 300:135-139.

Starkov AA, Chinopoulos C and Fiskum G (2004) Mitochondrial calcium and oxidative stress as mediators of ischemic brain injury. *Cell Calcium* 36: 257–264.

Stout AK, Raphael HM, Kanterewicz BI, Klann E and Reynolds IJ (1998) Glutamate-induced neuron death requires mitochondrial calcium uptake. *Nat Neurosci* 1:366-373.

Wang CN, Chi CW, Lin YL, Chen CF and Shiao YJ (2001) The neuroprotective effects of phytoestrogens on amyloid beta protein-induced toxicity are mediated by abrogating the activation of caspase cascade in rat cortical neurons. *J Biol Chem* 276:5287-5295.

Wang KK (2000) Calpain and caspase: can you tell the difference? *Trends Neurosci* 23:20-26.

White RJ and Reynolds IJ (1996) Mitochondrial depolarization in glutamate-stimulated neurons: an early signal specific to excitotoxin exposure. *J Neurosci* 16:5688-5697.

Yu SW, Wang H, Poitras MF, Coombs C, Bowers WJ, Federoff HJ, Poirier GG, Dawson TM and Dawson VL (2002) Mediation of poly(ADP-ribose) polymerase-1-dependent cell death by apoptosis-inducing factor. *Science* 297:259-263.

Zhang Z, Leonard SS, Huang C, Vallyathan V, Castranova V and Shi X (2003) Role of reactive oxygen species and MAPKs in vanadate-induced G(2)/M phase arrest. *Free Radic Biol Med* 34:1333-1342.

Footnotes

This study was supported by Grant NRICM-93-2323-B-077-001 from National Science Council, and Grants 94DBCMR-2 and 94DBCMR-3 from National Research Institute of Chinese medicine, Taiwan, R.O.C.

Reprint requests received by

Dr. Young-Ji Shiao

National Research Institute of Chinese Medicine

NO. 155-1. Sec. 2, LiNung ST., Peitou, Taipei, Taiwan, R.O.C.

E-mail: yshiao@nricm.edu.tw

Molecular Pharmacology Fast Forward. Published on December 19, 2005 as DOI: 10.1124/mol.105.018770
This article has not been copyedited and formatted. The final version may differ from this version.

Legends for figures

Fig. 1. The structure of tournefolic acid B (TAB), tournefolic acid B methyl ester (TABM), and tournefolic acid B ethyl ester (TABE).

Fig. 2. TABM and TABE decreased NMDA-mediated cell death. Cortical neurons were treated with vehicle (0.1% DMSO, v/v) or 10-100 μM TAB (A), TABM (B), or TABE (C) for 30 min. After then, NMDA was added to a final concentration of 50 μM and incubated for 24 h. Cell viability was measured by MTT reduction. Cells were treated with vehicle, 50 μM TAB, TABM, or TABE for 30 min then challenged without (opened column) or with (closed column) 50 μM NMDA for 24 h. Cell viability was measured by LDH release (D). Results are means ± S.D. from five independent experiments for MTT reduction and four independent experiments for LDH release, and are expressed relative to control cells for MTT reduction, and relative to the intracellular LDH in control cells for LDH release. Significant differences between cells treated with NMDA and NMDA plus TAB derivatives are indicated by *, $p < 0.05$; ** $p < 0.01$; and *** $p < 0.001$. Panel E are the representative photographs of MAP-2 immunofluorescent staining of neurons. Cells were treated with vehicle (a, d), 50 μM TABM (b, e), or 50 μM TABE (c, f) for 30 minutes then exposed to 50 μM NMDA for 0 (a-c) and 4 h (d-f).

Molecular Pharmacology Fast Forward. Published on December 19, 2005 as DOI: 10.1124/mol.105.018770
This article has not been copyedited and formatted. The final version may differ from this version.

Fig. 3. NMDA activated calpain and caspase 3. Cortical neurons were incubated with 50 μM NMDA for 0-30 h. Equal amount of cell lysate was subjected to immunobloting using anti-α-spectrin antibody. Panel A are the representative immunoblots of α-spectrin and degraded fragments. The activation of calpain cleaved 250 KDa α-spectrin (B) to produce 150 (C) and 145 KDa (D) fragments, whereas activation of caspase 3 generated 120 (E) and 150 KDa fragments of α-spectrin. Results are means ± S.D. (where large enough to be shown) from three independent experiments, and are expressed relative to control cells for 250 KDa, or relative to cells treated with MNDA for 30 h for 150, 145, and 120 KDa. Significant differences between control cells and cells treated with NMDA are indicated by *, $p < 0.05$; ** $p < 0.01$; and *** $p < 0.001$.

Fig. 4. TABM and TABE attenuated NMDA-mediated activation of caspase 3. Cortical neurons were incubated with vehicle (opened column), 50 μM TABM (closed column), or 50 μM TABE (dotted column) for 30 min then challenged with 50 μM NMDA for 0-24 h. Immunobloting was performed using anti-α-spectrin antibody to detect 250 KDa (B) α-spectrin or 150 (C), 145 (D), and 120 KDa (E) degraded fragments of α-spectrin. Panel A are the representative immunoblots of α-spectrin and degraded fragments. Results are means ± S.D. (where large enough to be shown) from four independent experiments, and are expressed relative to cells at zero time-point for 250 KDa, or relative to cells treated

with MNDA for 24 h for 150, 145, and 120 KDa. Significant differences between cells treated with NMDA alone and cells treated with NMDA plus TABM or TABE are indicated by *, $p < 0.05$; ** $p < 0.01$; and ***, $p < 0.001$.

Fig. 5. TABM and TABE attenuated the NMDA-induced increase of caspases activities. Cells were treated with NMDA for 0-24 h (A). Cells were harvested to assay the activity of caspase 2 (opened column), 3 (closed column), 6 (dotted column), 8 (hatched column), and 9 (cross hatched column). Results are means ± S.D. (where large enough to be shown) from three independent experiments. Significant differences between control cells and cells treated with NMDA are indicated by *, $p < 0.05$; **, $p < 0.01$; and ***, $p < 0.001$. Cells were treated with vehicle (opened column), 50 μM TABM (closed column), or 50 μM TABE (dotted column) for 30 min then exposed to 50 μM NMDA for 8 h (B). Cells were harvested to assay the activity of caspase 2, 3, 6, 8, and 9. Results are means ± S.D. (where large enough to be shown) from five independent experiments. Significant differences between cells treated with NMDA and cells treated with NMDA plus TAB ester derivative are indicated by **, $p < 0.01$; and ***, $p < 0.001$.

Fig. 6. TABM and TABE attenuated the activation of caspase 12 induced by NMDA. Cells were treated with 50 μM NMDA for 0-24 h (A). Equal amount of cell lysate was

Molecular Pharmacology Fast Forward. Published on December 19, 2005 as DOI: 10.1124/mol.105.018770
This article has not been copyedited and formatted. The final version may differ from this version.

subjected to immunobloting using anti-caspase 12 antibody to detect the level of 55 KDa (opened column) and 40 KDa (closed column) procaspase 12. Cells were treated with vehicle, 50 μM TABM, or 50 μM TABE for 30 min then exposed to 50 μM NMDA for 8 h (B). Equal amount of cell lysate was subjected to immunobloting using anti-caspase 12 antibody. Activation of caspase 12 induced the cleavage of 40 KDa procaspase 12. Results are means ± S.D. from four independent experiments, and are expressed relative to control cells. The top parts of each panel are the representative immunoblots of 55 KDa and 40 KDa procaspase 12. Significant differences between control cells and cells treated with NMDA are indicated by *, $p < 0.05$; and ***, $p < 0.001$. Significant differences between cells treated with NMDA and cells treated with NMDA plus TAB ester derivative are indicated by †, $p < 0.05$; and ††, $p < 0.01$.

Fig. 7. TABM and TABE diminished the NMDA-mediated $O_2^{\bullet-}$ accumulation. Cells were exposed to 50 μM NMDA for 0-8 h (A). Cells were treated with vehicle, 50 μM TABM, or 50 μM TABE for 30 min, then incubated without or with 50 μM NMDA for 20 min (B). The level of intracellular $O_2^{\bullet-}$ was measured by dihydroethidium assay. Results are means ± S.D. from four independent experiments, and are expressed relative to control cells. Significant differences between control cells and cells treated with NMDA in panel A, or

Molecular Pharmacology Fast Forward. Published on December 19, 2005 as DOI: 10.1124/mol.105.018770
This article has not been copyedited and formatted. The final version may differ from this version.

between cells treated with NMDA and cells treated with NMDA plus TABM or TABE in panel B are indicated by ***, $p < 0.001$.

Fig. 8. The effects of TABM and NMDA on the mitochondrial membrane potential. Cells were loaded with TMRM to monitor the mitochondrial membrane potential. TMRM-loaded cells were transferred to a microscope-equipped humidity chamber in a condition of 37°C and 5% CO_2. Cells were exposed to 50 μM NMDA (opened column) or 50 μM TABM (closed column) at 3 min time-point and detected by fluorescence microscope with excitation wavelength 555 nm. The time-lapse images during 30 min were captured every 15 sec using MetaFluor software. Results are means ± S.D. from four independent experiments, and are expressed relative to cells at the first recording time-point. Panel A and B are the representative time-course of TMRM fluorescence recorded in cells treated with 50 μM NMDA and 50 μM TABM, respectively. Panel C is the relative average of fluorescence intensity in cells treated with NMDA or TABM. Panel D is the relative fluorescence intensity in cells treated with NMDA or TABM for 0, 0.5, 7, 17, and 27 min. Significant differences between cells treated with NMDA and TABM are indicated by **, $p < 0.01$.

Molecular Pharmacology Fast Forward. Published on December 19, 2005 as DOI: 10.1124/mol.105.018770
This article has not been copyedited and formatted. The final version may differ from this version.

Fig. 9. Effect of TABM on the NMDA-induced elevation of $[Ca^{2+}]_i$. Cells were loaded with fluo-3 AM to monitor the level of $[Ca^{2+}]_i$. Fluo-3 AM-loaded cells were treated with vehicle (opened column) or 50 μM TABM (closed column) for 30 min then transferred to a microscope-equipped humidity chamber in a condition of 37°C and 5% CO_2. Cells were exposed to 50 μM NMDA at 1 min time-point and detected by fluorescence microscope with excitation wavelength 484 nm. The time-lapse images during 60 min were captured using MetaFluor software. Results are means ± S.D. from four independent experiments. Panel A and B are the representative time-course of Ca^{2+}-dependent fluorescence recorded in control cells and TABM-treated cells, respectively. Panel C is the average of time-course effect of TABM on the NMDA-induced elevation of fluorescence. Panel D is the fluorescence intensity at 0, 5, 30, and 60 min. Significant differences between cells treated with NMDA and cells treated with NMDA plus TABM are indicated by **, $p < 0.01$; and ***, $p < 0.001$.

Fig. 10. TABM eliminated the NMDA-induced elevation of $[Ca^{2+}]_{er}$. . Cells were loaded with mag-fura-2 AM to monitor the level of $[Ca^{2+}]_{er}$. Mag-fura-2 AM-loaded cells were treated with vehicle (opened column) or 50 μM TABM (closed column) for 30 min then transferred to a microscope-equipped humidity chamber in a condition of 37°C and 5% CO_2. Cells were exposed to 50 μM NMDA at 1 min time-point and detected by

fluorescence microscope with dual excitation wavelength 340 and 380 nm. The time-lapse images during 60 min were captured using MetaFluor software. Results are means ± S.D. from four independent experiments. Panel A and B are the representative time-course of ratiometric values (Ex340 nm/Ex380 nm) in control cells and TABM-treated cells, respectively. Panel C is the average of time-course effect of TABM on the NMDA-induced elevation of ratiometric value. Panel D is the ratiometric value at 0, 5, 30, and 60 min. Significant differences between cells treated with NMDA and cells treated with NMDA plus TABM are indicated by **, $p < 0.01$.

Fig. 11. TABM eliminated the NMDA-induced elevation of $[Ca^{2+}]_{mit}$. Cells were loaded with rhod-2 AM to monitor the level of $[Ca^{2+}]_{mit}$. Rhod-2 AM-loaded cells were treated with vehicle (opened column) or 50 μM TABM (closed column) for 30 min then transferred to a microscope-equipped humidity chamber in a condition of 37°C and 5% CO_2. Cells were exposed to 50 μM NMDA at 1 min time-point and detected by fluorescence microscope with excitation wavelength 555 nm. The time-lapse images during 60 min were captured using MetaFluor software. Results are means ± S.D. from four independent experiments (where large enough to be shown). Panel A and B are the representative time-course of Ca^{2+}-dependent fluorescence recorded in control cells and TABM-treated cells, respectively. Panel C is the average of time-course effect of TABM

Molecular Pharmacology Fast Forward. Published on December 19, 2005 as DOI: 10.1124/mol.105.018770
This article has not been copyedited and formatted. The final version may differ from this version.

on the NMDA-induced elevation of fluorescence. Panel D is the fluorescence intensity at 0, 5, 30, and 60 min. Significant differences between cells treated with NMDA and cells treated with NMDA plus TABM are indicated by **, $p < 0.01$; and ***, $p < 0.001$.

Molecular Pharmacology Fast Forward. Published on December 19, 2005 as DOI: 10.1124/mol.105.018770
This article has not been copyedited and formatted. The final version may differ from this version.

Fig. 1.

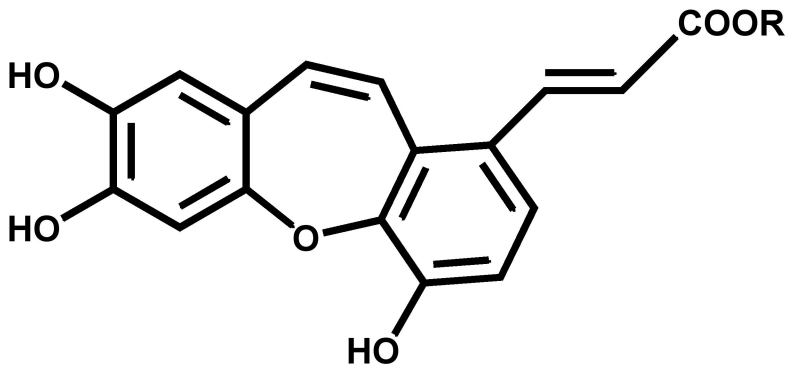

R=H, Tournefolic acid B (TAB)

R= CH_3, Tournefolic acid B methyl ester (TABM)

R=CH_2CH_3, Tournefolic acid B ethyl ester (TABE)

Molecular Pharmacology Fast Forward. Published on December 19, 2005 as DOI: 10.1124/mol.105.018770
This article has not been copyedited and formatted. The final version may differ from this version.

Fig. 2.

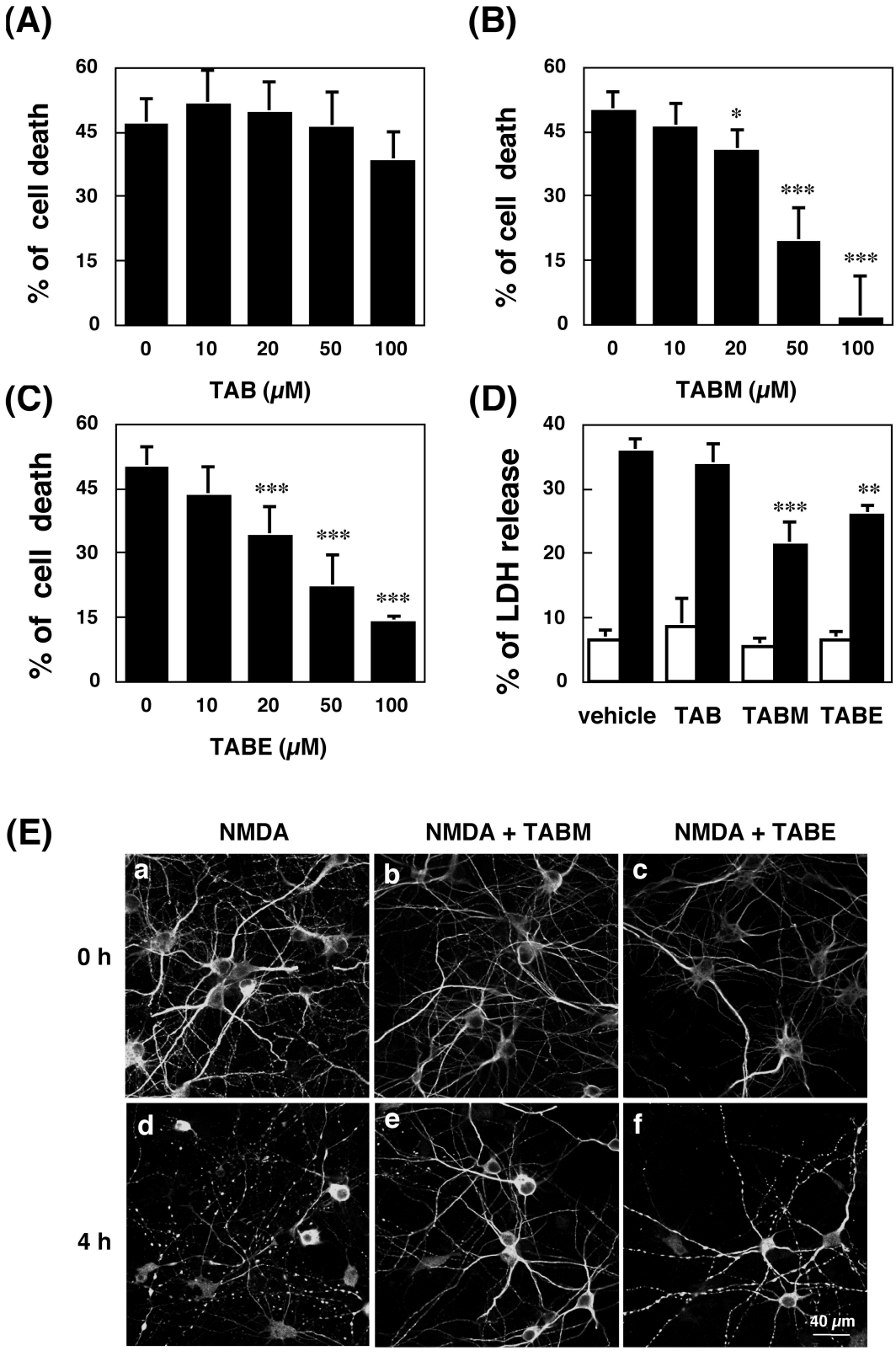

Molecular Pharmacology Fast Forward. Published on December 19, 2005 as DOI: 10.1124/mol.105.018770
This article has not been copyedited and formatted. The final version may differ from this version.

Fig. 3.

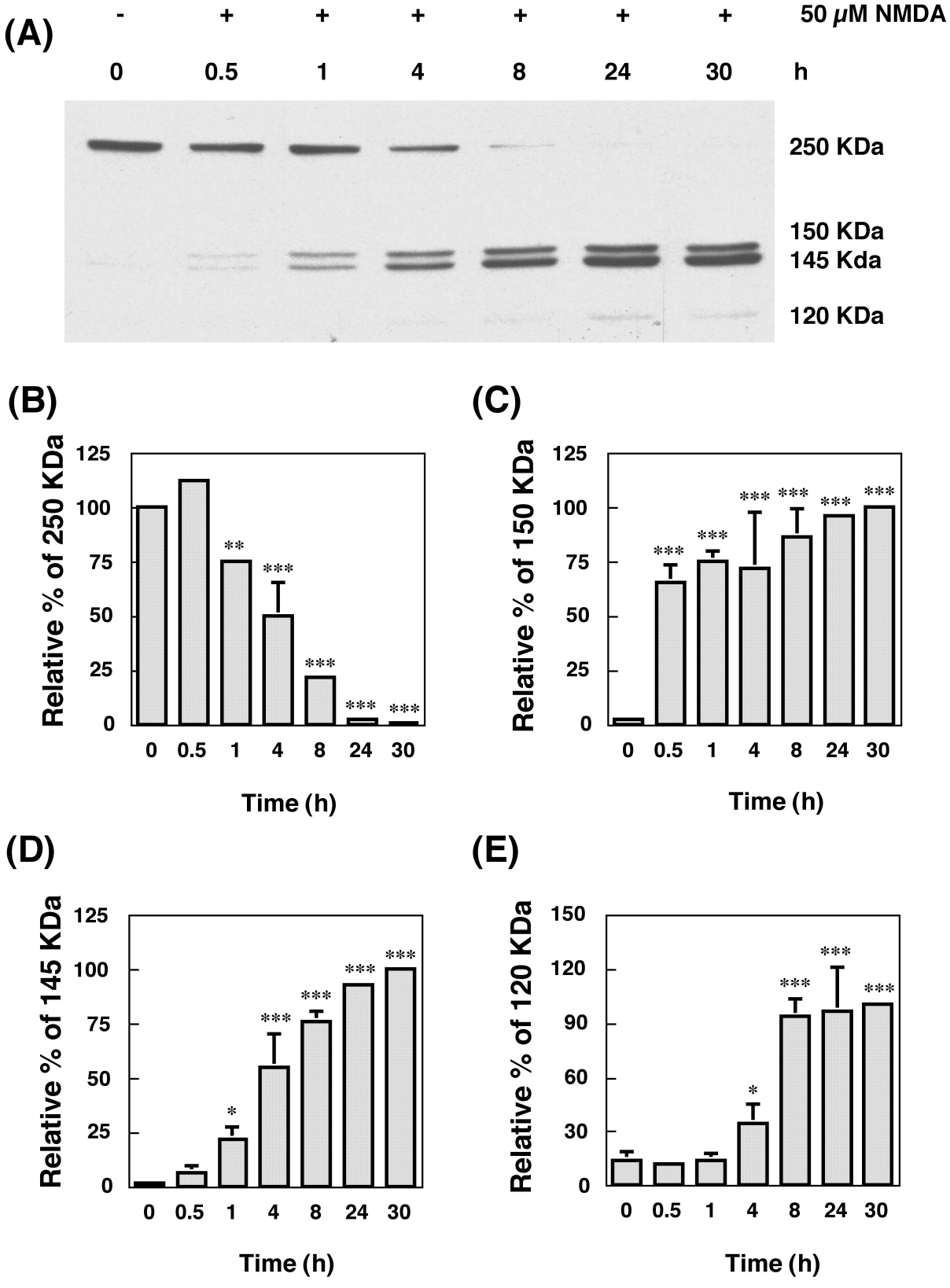

Molecular Pharmacology Fast Forward. Published on December 19, 2005 as DOI: 10.1124/mol.105.018770
This article has not been copyedited and formatted. The final version may differ from this version.

Fig. 4.

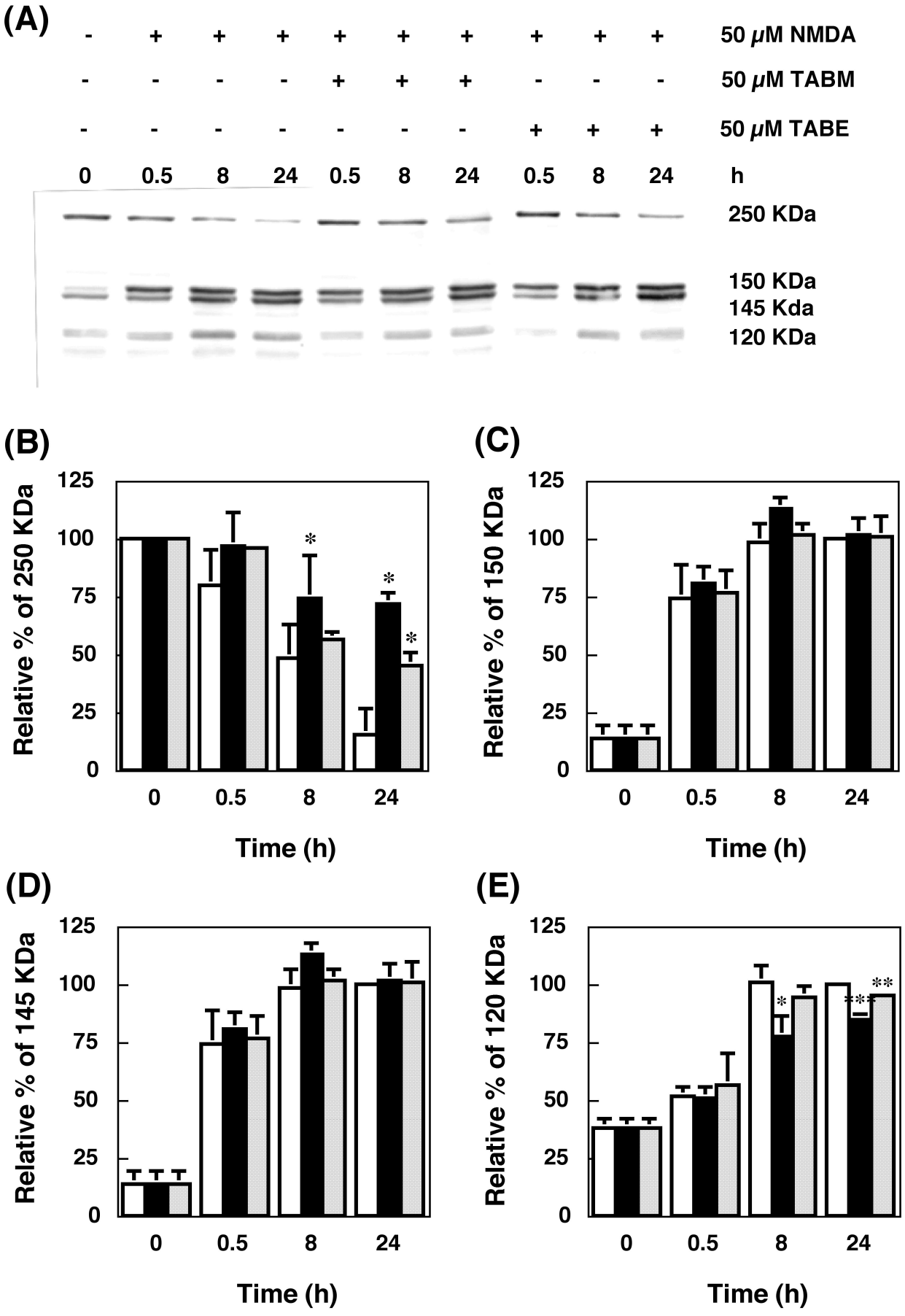

Molecular Pharmacology Fast Forward. Published on December 19, 2005 as DOI: 10.1124/mol.105.018770
This article has not been copyedited and formatted. The final version may differ from this version.

Fig 5

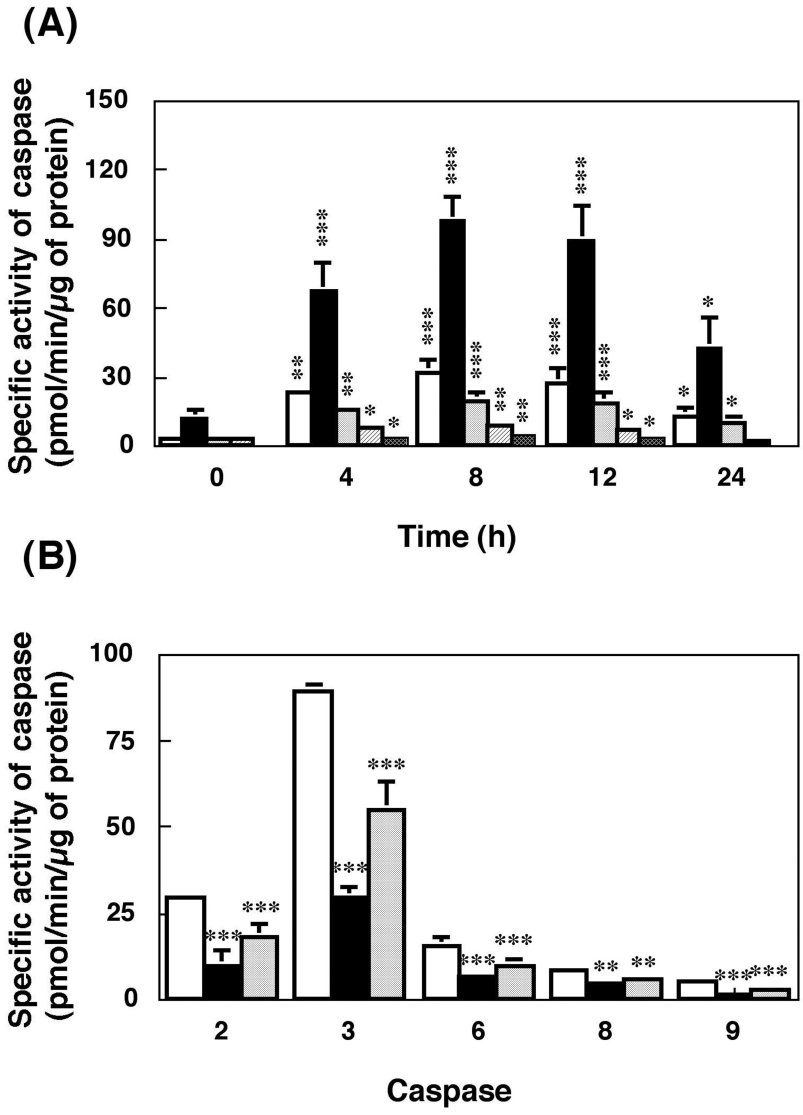

Molecular Pharmacology Fast Forward. Published on December 19, 2005 as DOI: 10.1124/mol.105.018770
This article has not been copyedited and formatted. The final version may differ from this version.

Fig. 6.

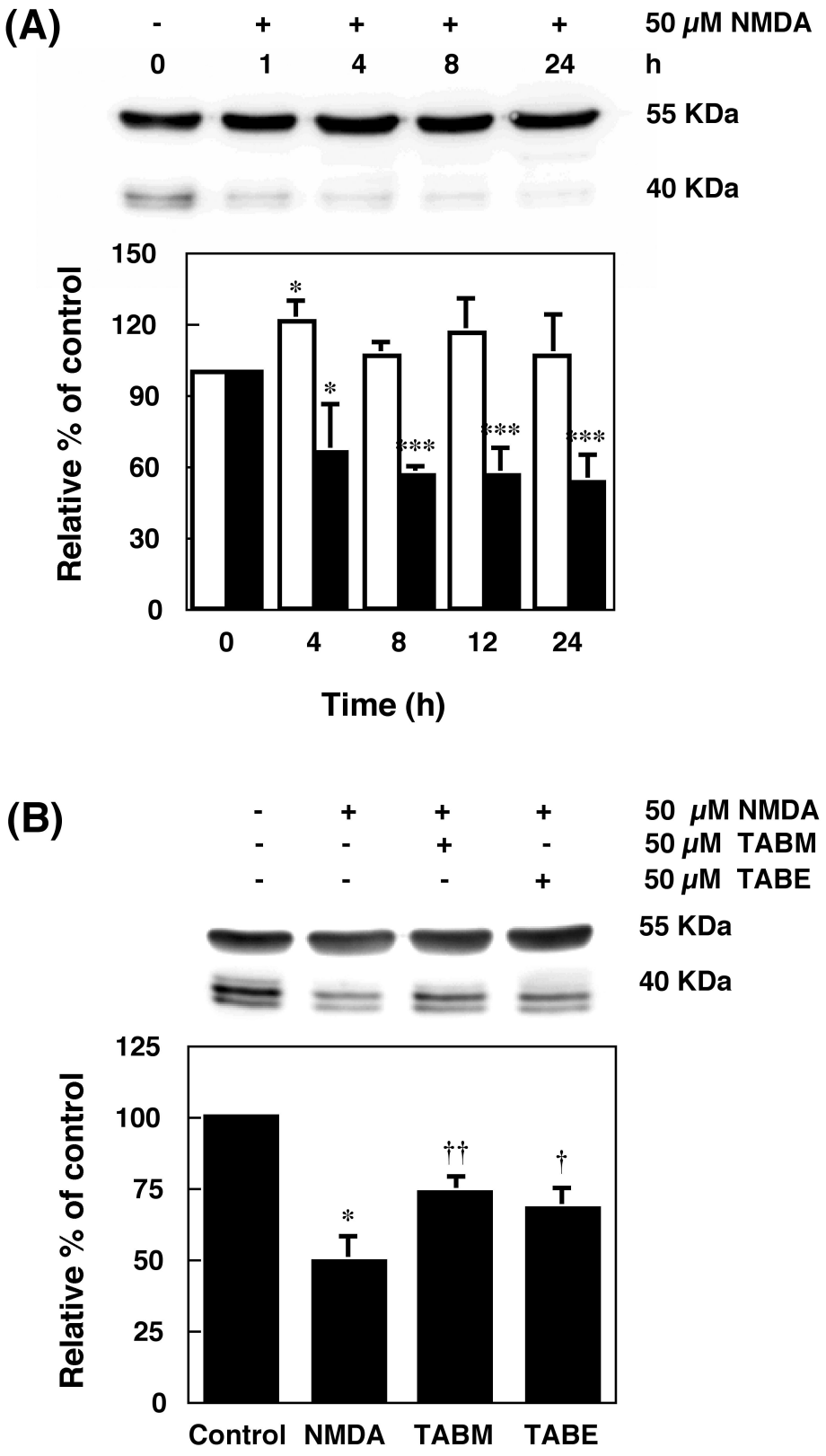

Molecular Pharmacology Fast Forward. Published on December 19, 2005 as DOI: 10.1124/mol.105.018770
This article has not been copyedited and formatted. The final version may differ from this version.

Fig. 7.

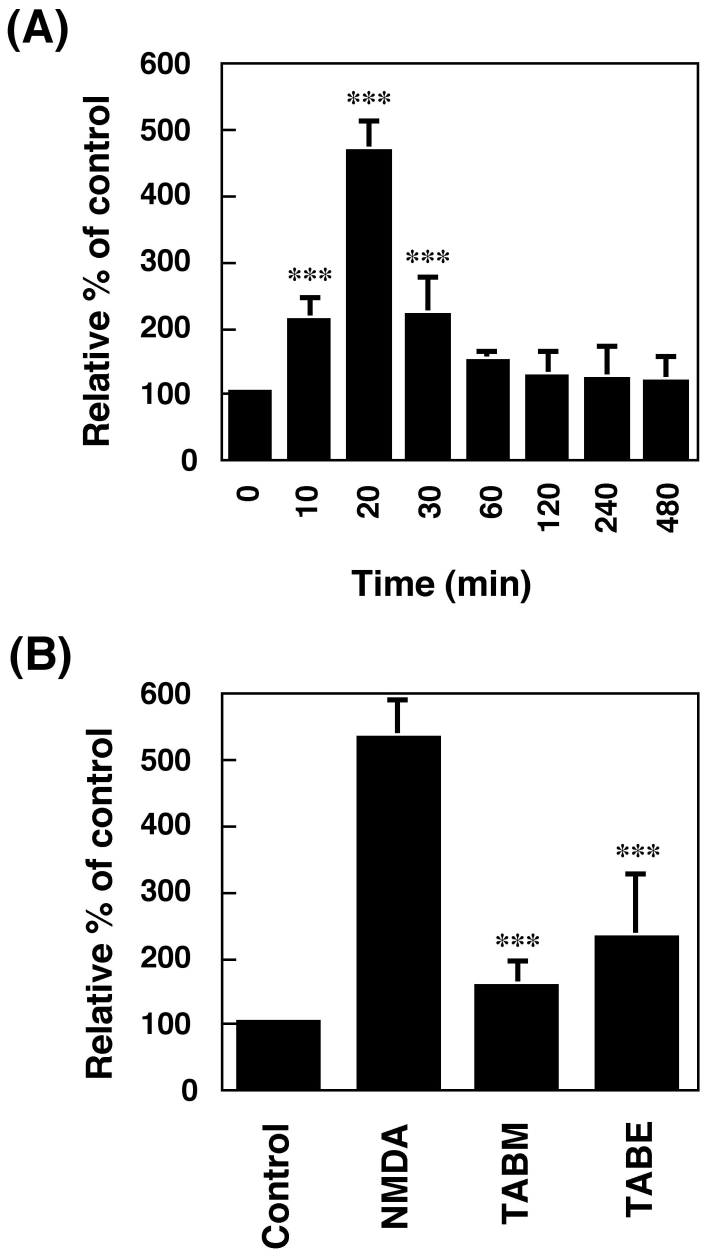

Molecular Pharmacology Fast Forward. Published on December 19, 2005 as DOI: 10.1124/mol.105.018770
This article has not been copyedited and formatted. The final version may differ from this version.

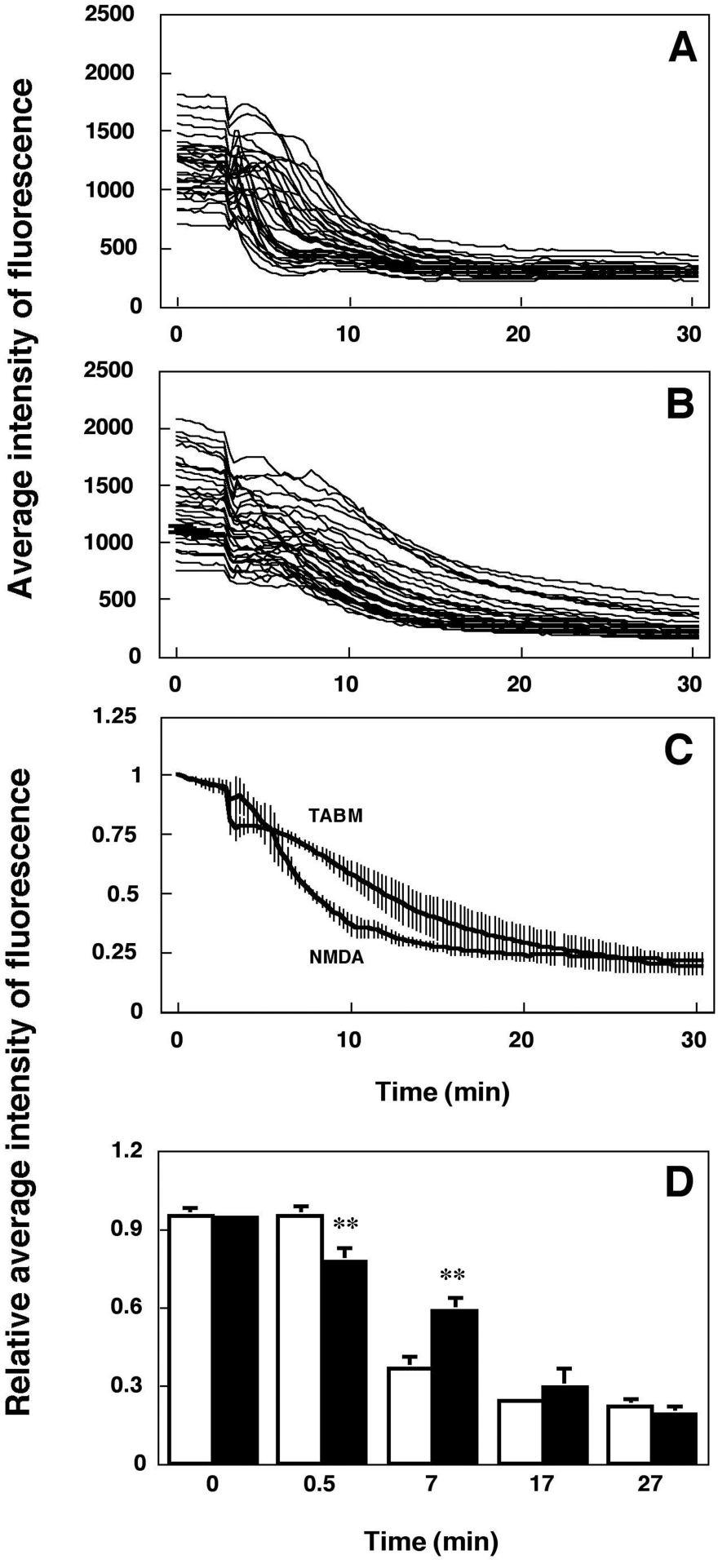

Molecular Pharmacology Fast Forward. Published on December 19, 2005 as DOI: 10.1124/mol.105.018770
This article has not been copyedited and formatted. The final version may differ from this version.

Fig 9

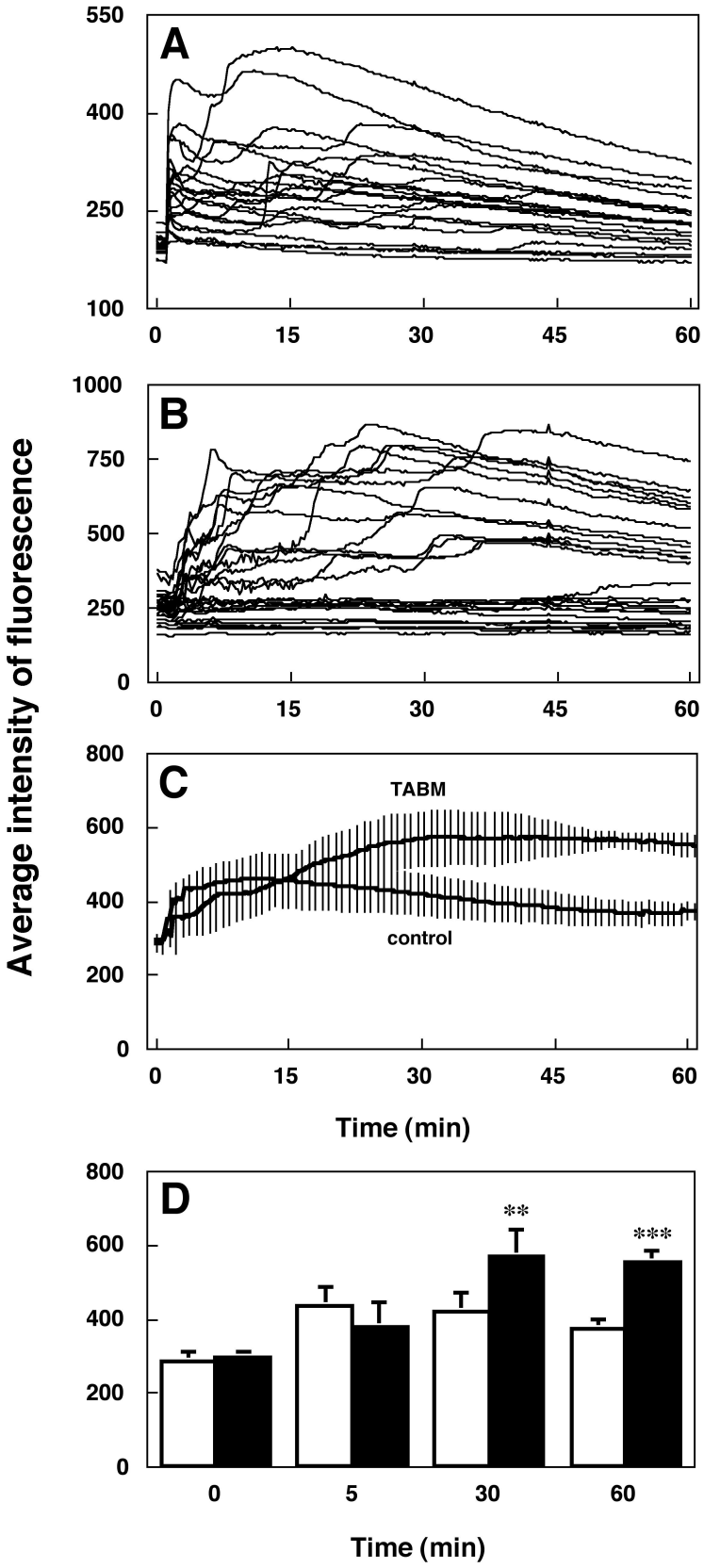

Molecular Pharmacology Fast Forward. Published on December 19, 2005 as DOI: 10.1124/mol.105.018770
This article has not been copyedited and formatted. The final version may differ from this version.

Fig 10

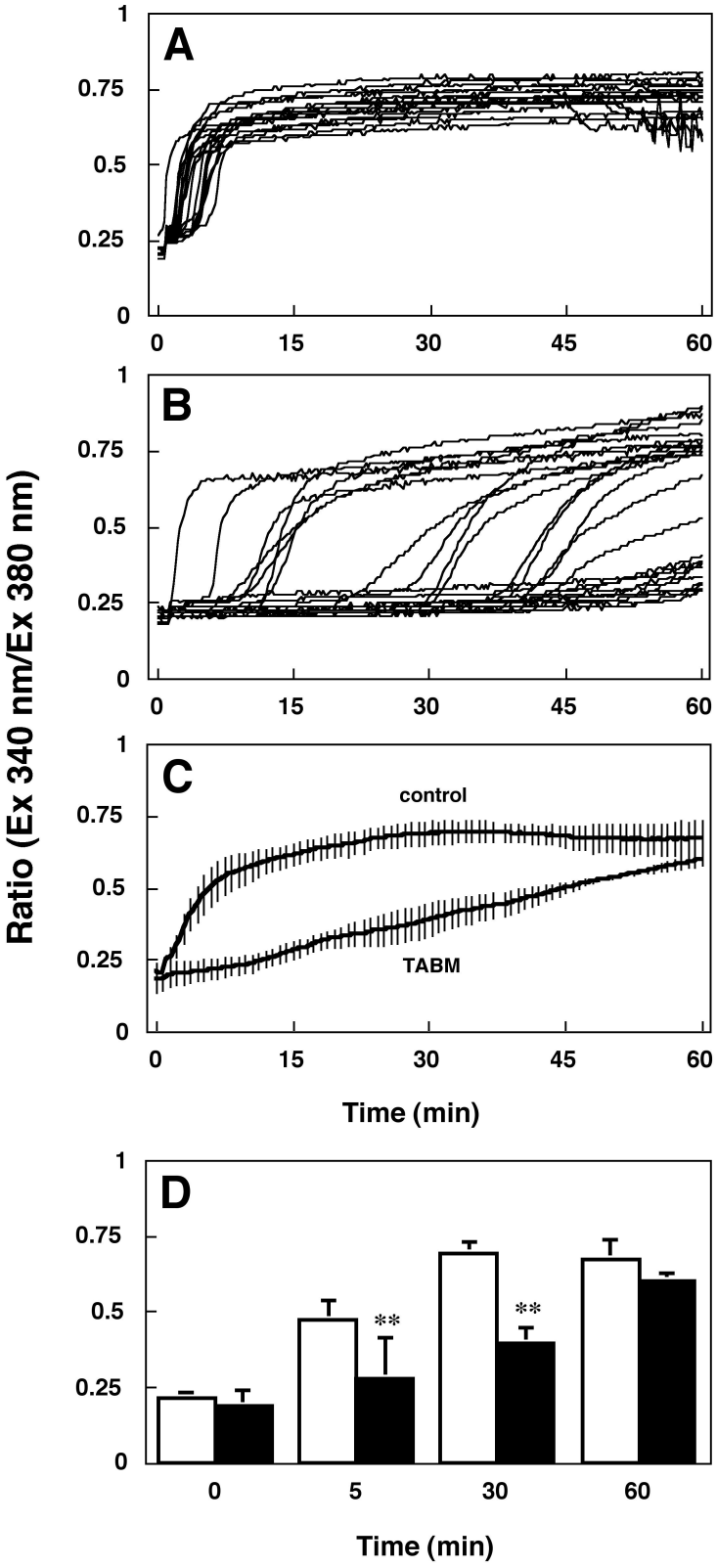

Molecular Pharmacology Fast Forward. Published on December 19, 2005 as DOI: 10.1124/mol.105.018770
This article has not been copyedited and formatted. The final version may differ from this version.

F ig 11